ELSEVIER

Short communication

Electrochemical properties of cobalt-exchanged spinel lithium manganese oxide

S.H. Chang [a], K.S. Ryu [a], K.M. Kim [a], M.S. Kim [b], I.K. Kim [b], S.G. Kang [a, *]

[a] *Electronics and Telecommunications Research Institute, Telecommunication Basic Research Laboratory, Yusong P.O. Box 106, Taejon, 305-600, South Korea*
[b] *Wonkwang University, Department of Chemistry, Iksan, Jeonbuk, 570-749, South Korea*

Abstract

Cobalt-exchanged $LiCo_yMn_{2-y}O_4$ ($y = 0.0, 0.1, 0.2, 0.3, 0.4, 0.5$) is prepared at 800°C in air. The crystal symmetry of the $LiCo_yMn_{2-y}O_4$ is determined as cubic spinel with space group *Fd3m*. The lattice parameter and the discharge capacity decrease with increase in substituted Co content, but the cycle performance is enhanced. The first discharge capacity of $LiCo_{0.2}Mn_{1.8}O_4$ is 96 mAh g^{-1} in the 3.7–4.3 V range and 109 mAh g^{-1} in the 3.7–5.1 V range. A Mn(II) peak is observed in the cyclic voltammogram for spinel $LiMn_2O_4$. It is difficult to remove this Mn(II) with conventional preparation methods. The peak disappears in cobalt-exchanged spinel sample, $LiCo_yMn_{2-y}O_4$ ($y > 0.1$), and the cycle performance is enhanced. © 1999 Elsevier Science S.A. All rights reserved.

Keywords: Lithium secondary battery; Cathode materials; $LiMn_2O_4$; $LiCo_yMn_{2-y}O_4$

1. Introduction

Lithium manganese oxide is attractive as a positive electrode for lithium secondary batteries because of its low cost and environmental merits. Several authors [1–4] showed the possibility of electrochemical intercalation and de-intercalation of lithium reversibly to/from $LiMn_2O_4$ in the voltage range 3–4.1 V. The mechanism of lithium-ion insertion into the λ-MnO_2 structure was studied by Kanzaki et al. [5]. The process of second lithium intercalation around 3 V has also been investigated in the spinel structure ($LiMn_2O_4 \rightarrow Li_2Mn_2O_4$) [6,7]. Recently, the process around 4.1 V ($LiMn_2O_4 \rightarrow \lambda$-$MnO_2$) which corresponds to de-intercalation of lithium in the initial spinel structure has been studied [8]. In lithium-ion batteries, the lifecycle of $LiMn_2O_4$ synthesized at 600 to 900°C is inferior to that of $LiCoO_2$. According to studies of the non-stoichiometry of the spinel or partially substituted manganese oxide phase, Jahn–Teller distortion is induced at the end of charging to

3.5 V due to Mn(III). This distortion leads to rapid loss in capacity. In order to improve the cycle performance of $LiMn_2O_4$, the influence of the synthesis conditions and the non-stoichiometry of $LiMn_2O_4$ has been actively studied. It has been suggested [9] that optimum heat treatment is carried out at 650 to 750°C for 75 to 200 h. The composition of lithium ($Li_xMn_2O_4$) and the synthetic condition affect both the structure and the physicochemical properties. A partially inverse spinel structure induces capacity loss during the cycles in the high voltage region (4.45 and 4.95 V) [10,11]. Accordingly, the lifecycle of spinel $LiMn_2O_4$ is less than that of layered compounds such as $LiCoO_2$ and $LiNiO_2$.

To improve the cycle performance of $LiMn_2O_4$, substituted spinel phases of $LiM_yMn_{2-y}O_4$ (M = Ti, Ge, Fe, Co, Zn, etc.) have been examined extensively [4,8,12–15]. At $y \leq 0.25$ in $LiM_yMn_{2-y}O_4$, no change in the charge curve is observed during de-intercalation in the range 3.5–4.4 V and the cell capacity is maintained with cycling. By contrast, cell capacities are drastically decreased with highly substituted phases ($y > 0.25$).

In this study, cobalt-exchanged $LiCo_yMn_{2-y}O_4$ is prepared as a means to improve cycle performance. The structural properties for $LiCo_yMn_{2-y}O_4$ are investigated,

---

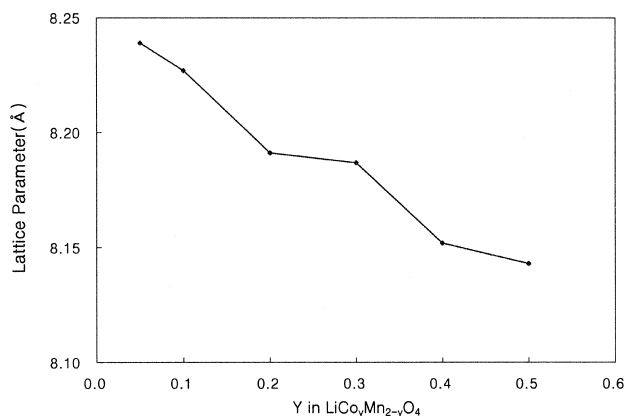* Corresponding author. Tel.: + 82-42-860-5998; fax: + 82-42-860-6836; E-mail: kangsg@etri.re.kr

Fig. 1. Lattice parameter for $LiCo_yMn_{2-y}O_4$.

and the cycle performance is examined in the range 3.7–5.1 V.

2. Experimental

Spinel $LiCo_yMn_{2-y}O_4$ ($y = 0$, 0.1, 0.2, 0.3, 0.4, 0.5) compounds were prepared by a conventional solid-state reaction using a mixture of LiOH, Co_3O_4 and chemically produced manganese dioxide (CMD). The mixtures were sintered at 800°C for 36 h in air with intermittent grinding and then were cooled to room temperature at a cooling rate of 50°C/h.

X-ray diffraction patterns were recorded by means of a MAC Science MXP 18 XRF diffractometer with Ni-filtered Cu Kα radiation and step scanning (0.02°) in the 2θ range from 10 to 100°. Rietveld refinement was made with the DBW 3.2S program.

The valence state of manganese ion was investigated by X-ray photoelectron spectroscopy (XPS). XPS spectra were obtained by means of a ESCA-LAB 200R, VG Scientific spectrometer. A Mg Kα X-ray source (1253.6 eV) was used. The base pressure of the sample chamber in the spectrometer was lower than 10^{-9} Torr. All binding energies were corrected with the carbon 1s line at 284.5 eV.

To investigate the electrochemical properties of $LiCo_yMn_{2-y}O_4$, electrochemical cells were assembled and consisted of $LiCo_yMn_{2-y}O_4$ as the positive electrode, Li metal as the negative electrode, and 1 M $LiPF_6$ dissolved in a 2:1 (volume ratio) mixture of ethylene carbonate (EC) and dimethyl carbonate (DMC) as the electrolyte. The cathode was mixture of 89 wt.% active material, 10 wt.% acetylene black, and 1 wt.% polytetrafluoroethylene (PTFE) binder. The cells were assembled in an argon-filled dry box. Cyclic voltammograms were obtained with a MacPile-II potentiostat system under a constant scan rate of 10 mV h^{-1} in the range 3.7–5.1 V. Galvanostatic measurements were performed at a constant current density (200 μA cm^{-2}) in the range from 3.5 to 4.3 V for the lower voltage region and 4.3 to 5.1 V for the higher voltage region.

3. Results and discussion

X-ray diffraction patterns for $LiCo_yMn_{2-y}O_4$ have been indexed to cubic symmetry (*Fd3m*). The lattice parameter decreased with increase in substituted Co content due to the small size of Co^{3+} ion (high spin ($t_{2g}^4e_g^2$) $r = 0.61$ Å, low spin ($t_{2g}^6e_g^0$) $r = 0.545$ Å) and a reduction in the Jahn–Teller effect (Fig. 1). High spin Mn^{3+} ($t_{2g}^3e_g^1$, $r = 0.645$ Å) induced Jahn–Teller distortion in the $LiCo_yMn_{2-y}O_4$. As the amount of Mn^{3+} in the spinel $LiCo_yMn_{2-y}O_4$ is decreased by substituting with Co^{3+} ions, the Jahn–Teller effect due to Mn^{3+} ions is reduced.

In order to confirm the redox reaction of $LiCo_yMn_{2-y}O_4$ during the charge–discharge process, low scan-rate potentiostatic measurements using a two-electrode configuration were performed (Fig. 2). The potential was swept between 3.7 and 4.3 V at a scan rate of 10 mV h^{-1}. A pair of separated redox peaks was observed at 4.05 and 4.15 V. This implies that the lithium intercalation–de-intercalation reaction proceeded via two steps during the electrochemical reaction. The peak intensities decreased rapidly with increasing Co content in the spinel $LiCo_yMn_{2-y}O_4$. The
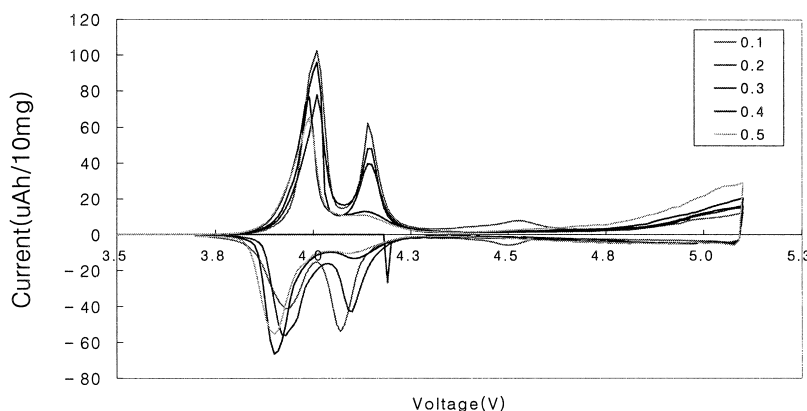

Fig. 2. Cyclic voltammogram for Li //$LiCo_yMn_{2-y}O_4$ cell (scan rate = 10 mV h^{-1}).

peak at 4.55 V due to the reversible redox reaction of Mn^{2+} in impurities such as MnO disappeared with Co substitution. This phenomenon indicates that Co substitution improves the stoichiometry of $LiCo_yMn_{2-y}O_4$.

The first charge and discharge curves for $LiCo_yMn_{2-y}O_4$ are shown in Fig. 3. Two plateaux, at 4.05 and 4.15 V, are observed in $LiMn_2O_4$ ($y = 0$). These are caused by structural transition of lithium manganese oxide. The plateaux decrease with increasing Co content, which suggests that the structural transition is not occurring in the $LiCo_yMn_{2-y}O_4$. The first charge capacity of $LiCo_yMn_{2-y}O_4$ decreases with cobalt content, but the first discharge capacity of $LiCo_{0.2}Mn_{1.8}O_4$ is the largest one. This implies that cobalt substitution decreases the irreversible loss during the electrochemical reactions. Therefore, substituted Co ions stabilize the spinel structure of lithium manganese oxide.

The variation in the discharge capacity of $LiCo_yMn_{2-y}O_4$ over the range 3.7–4.3 V is plotted in Fig. 4. The discharge capacity increases up to $y = 0.3$ and decreases above $y = 0.3$. The cycle performance of $LiCo_yMn_{2-y}O_4$ is enhanced, however, in comparison with that of $LiMn_2O_4$ ($y = 0$). As shown in Fig. 4, $LiCo_{0.2}Mn_{1.8}O_4$ has better cycle performance and higher

Fig. 4. Variation of discharge capacity (3.7 to 4.3 V) for $Li\|LiCo_yMn_{2-y}O_4$ cell. Values of y given in inset.

discharge capacity than others. The first discharge capacity of $LiCo_{0.2}Mn_{1.8}O_4$ is 96 mA h^{-1} g (3.7 to 4.3 V). As the substitution of Co(III) for Mn in the spinel is increased, the average oxidation state of Mn is decreased. This means that the concentration of Mn(III), which induces the Jahn–Teller distortion in spinel, is decreased. Therefore,
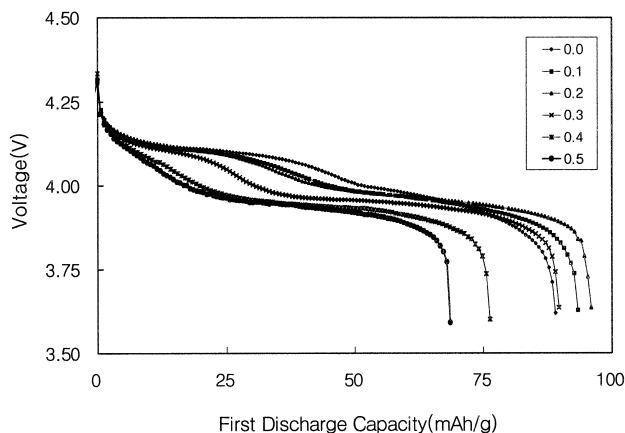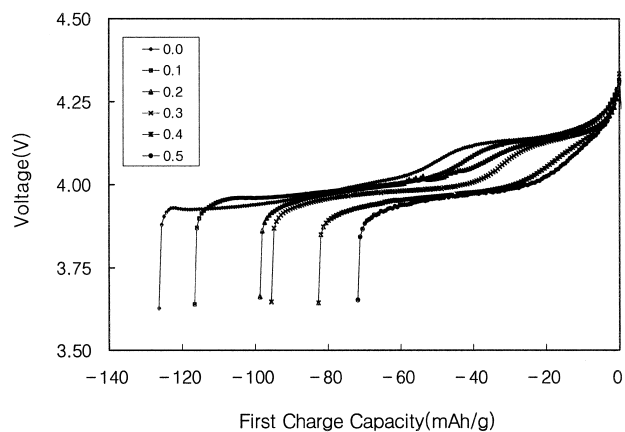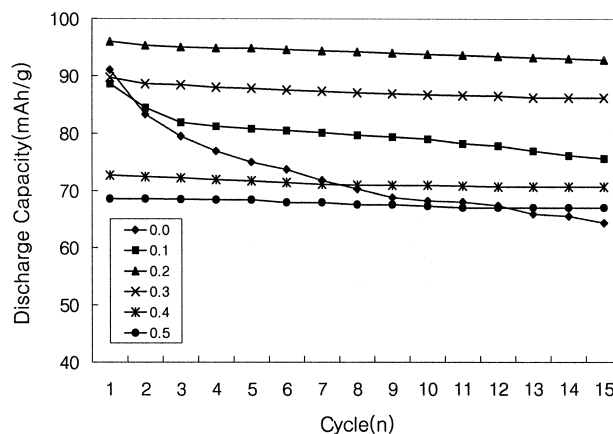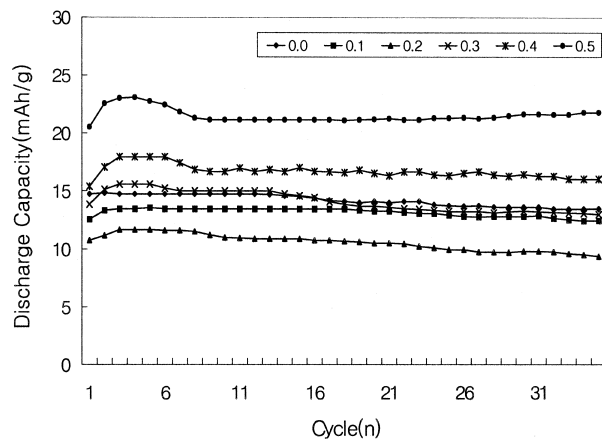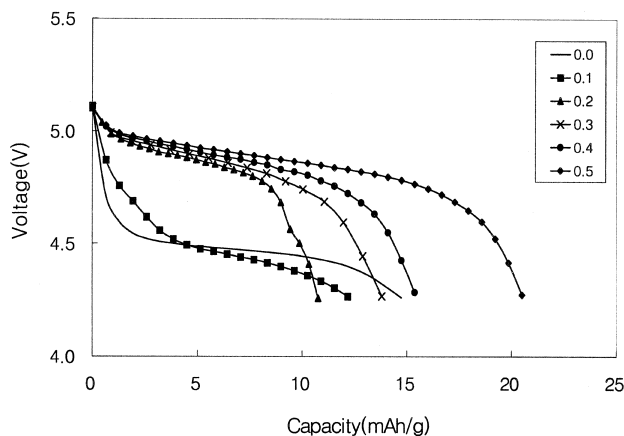

Fig. 3. First charge and discharge capacity (3.7 to 4.3 V) for $Li\|LiCo_yMn_{2-y}O_4$. Values of y given in inset.

Fig. 5. First discharge capacity and variation of discharge capacity (4.3 to 5.1 V) for $Li\|LiCo_yMn_{2-y}O_4$ cell. Values of y given in inset.
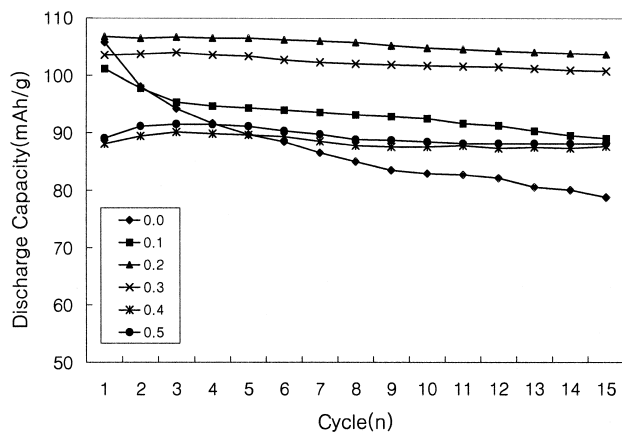
Fig. 6. Variation of discharge capacity (3.7 to 5.1 V) for Li‖LiCo$_y$Mn$_{2-y}$O$_4$ cell. Values of y given in inset.

the spinel structure of LiCo$_y$Mn$_{2-y}$O$_4$ is stabilized with Co substitution, so that the cycling stability is enhanced compared with the spinel LiMn$_2$O$_4$.

The first discharge curve and the capacity variation for the spinel LiCo$_y$Mn$_{2-y}$O$_4$ in the range 4.3–5.1 V are shown in Fig. 5. A reversible plateau at around 4.5 V is observed for LiMn$_2$O$_4$. Above LiCo$_{0.2}$Mn$_{1.8}$O$_4$ ($y = 0.2$), the plateau around 4.5 V disappears and a new reversible plateau appears at around 5.0 V. The latter plateau increases with Co content. This implies that the capacity for LiCo$_y$Mn$_{2-y}$O$_4$ ($y > 0.2$) in the range 4.3–5.1 V increases with Co content. The variation in discharge capacity for LiCo$_y$Mn$_{2-y}$O$_4$ in the range 3.7–5.1 V (Fig. 6) suggests that the reversibility of the charge–discharge cycle for LiCo$_y$Mn$_{2-y}$O$_4$ is improved without overall loss of energy in comparison with spinel LiMn$_2$O$_4$. This fact means that the structural stability of LiCo$_y$Mn$_{2-y}$O$_4$ due to Co substitution contributes to the reversibility of the charge–discharge cycle.

4. Conclusions

Cobalt-exchanged LiCo$_y$Mn$_{2-y}$O$_4$ has been prepared by a solid-state reaction at 800°C for 36 h in air. As Co ion substitution proceeds, the structure of LiCo$_y$Mn$_{2-y}$O$_4$ is stabilized due to diminution of Jahn–Teller distortion. The cycle performance of LiCo$_y$Mn$_{2-y}$O$_4$ is enhanced and LiCo$_{0.2}$Mn$_{1.8}$O$_4$ has good cycle performance and discharge capacity. The discharge capacity of LiCo$_{0.2}$Mn$_{1.8}$O$_4$ is 96 mAh g^{-1} for 3.7 to 4.3 V and 109 mAh g^{-1} for 3.7 to 5.1 V, respectively.

References

[1] J.M. Tarascon, D. Guyomard, J. Electrochem. Soc. 138 (1991) 2864.
[2] D. Guymark, J.M. Tarascon, J. Electrochem. Soc. 139 (1992) 937.
[3] M.M. Thackeray, W.I.F. David, P.G. Bruce, J.B. Goodenough, Mater. Res. Bull. 18 (1983) 461.
[4] M.M. Thackeray, P.J. Johnson, L.A. De Picciotto, P.G. Bruce, J.B. Goodenough, Mater. Res. Bull. 19 (1984) 179.
[5] Y. Kanzaki, A. Taniguchi, M. Abe, J. Electrochem. Soc. 138 (1991) 334.
[6] J.M. Tarascon, W.R. McKinnon, F. Coowar, T.N. Bowmer, G. Amatucci, D. Guymard, J. Electrochem. Soc. 141 (1994) 1421.
[7] T. Ohzuku, M. Kitugawa, T. Hirai, J. Electrochem. Soc. 137 (1990) 769.
[8] J.M. Tarascon, E. Wang, F.K. Shokoohi, W.R. Mackinon, S. Colson, J. Electrochem. Soc. 138 (1991) 2859.
[9] A. Momchilov, V. Manev, A. Nassalevska, A. Kozawa, J. Power Sources 41 (1993) 305.
[10] J.M. Tarascon, D. Guymard, Solid State Ionics 69 (1994) 222.
[11] J.M. Tarascon, D. Guymard, Solid State Ionics 69 (1994) 293.
[12] H. Tamura, K. Ishizerki, M. Nagayama, R. Furuichi, J. Electrochem. Soc. 141 (1994) 2035.
[13] L. Iguahua, H. Ikuta, T. Uchida, M. Wakihara, J. Electrochem. Soc. 143 (1996) 178.
[14] S.G. Kang, S.J. Hong, C.H. Yo, K.H. Jang, S.H. Chang, Bull. Korean Chem. Soc. 19 (1998) 265.
[15] M.S. Song, D.S. Ahn, S.G. Kang, S.H. Chang, Solid State Ionics 111 (1998) 237.